Prime number logarithmic geometry on the plane

Lubomir Alexandrov

JINR, LTP, Dubna 141980, Moscow Region, Russia

Abstract *We found a regularity of the behavior of primes that allows to represent both prime and natural numbers as infinite matrices with a common formation rule of their rows. This regularity determines a new class of infinite cyclic groups that permit the proposition a plane–spiral geometric concept of the arithmetic.*

1 Introduction

Counting arithmetic functions for different prime sets can be assigned to *the archaic mathematical reality.*

Nevertheless, the generated by them prime sequences, named *Eratosthenes progressions*, became known only in recent years (e.g.,[1],[2],[3] and sequences A007097, A063502, A064110 in [4]).

The Eratosthenes progression possesses a common formation law of its elements (an *inner prime number distribution law*) the realization of which is based on a multiple use of the Eratosthenes sieve [1] (Figure 1).

The derivation of Eratosthenes progressions and their systematic investigation is directed to a learning the nonasymptotic behaviour of primes, i.e., of the function's behaviour

$$d(n) = p(n+1) - p(n),\ n = 1, 2, \ldots, \overline{n},$$

where $p(n)$ is the nth prime and $\overline{n}$ is a sufficiently large natural number.

The inner prime number distribution law can be applied mostly in mathematics itself, for example, when constructing new geometric concepts in arithmetic.

Following Alain Connes ([5] pp. 208–209), it can be supposed that the specific behaviour of primes will reflect itself in the new geometry sought for understanding quantum gravity.

In biochemistry, the specific behaviour of primes can manifest itself in the laws of formation and functioning of large molecules, from 10^3–atomic insulin and hemoglobin up to $3 \cdot 10^5$–atomic proteins and enzymes.

In this paper, the general statement of the problem for derivation of Eratosthenes progressions is given and their basic properties are presented. The general results are applied to the sequence of primes itself

$$P = \{2, 3, 5, 7, 11, \ldots\} = \{p(n)\}_{n=1,2,\ldots},$$

as well as to the following related to P sequences:

$M = \mathbb{N} \backslash P = \{4, 6, 8, 9, \ldots\} = \{m(n)\}_{n=1,2,\ldots}$ the set of composite numbers;

$T = \{t(\nu) = (p(\nu), p(\nu+1)) : \nu \in \Lambda\}$ the set of twin pairs, where $\Lambda = \{n : p(n+1) - p(n) = 2, n \in \mathbb{N}\} = \{2, 3, 5, 7, 10, 13, 17, \ldots\}$;

$T_1 = \{p(\nu) : (p(\nu), p(\nu+1)) \in T, \nu \in \Lambda\} = \{t_1(\nu)\}_{\nu \in \Lambda}$ the set of first elements of twins;

$T_2 = \{p(\nu+1) : (p(\nu), p(\nu+1)) \in T, \nu \in \Lambda\} = \{t_2(n)\}_{\nu \in \Lambda}$ the set of second elements of twins;

$T_3 = T_1 \cup T_2 = \{3, 5, 7, 11, 13, 17, 19, \ldots\}$ the set of twin elements;

$S = P \setminus T_3 = \{2, 23, 37, 47, 53, \ldots\}$ the set of isolated primes[4], A007510;

$D_{6n-1} = \{6n - 1 \in P : n = 1, 2, \ldots,\} = \{5, 11, 17, \ldots\}$ the set of primes of the kind $6n - 1$;

$D_{6n+1} = \{6n + 1 \in P : n = 1, 2, \ldots,\} = \{7, 13, 19, \ldots\}$ the set of primes of the kind $6n + 1$, and

$T_4 = \{t(n) : (t_1(n) + t_2(n))/2 = 6 \cdot q, q \in P\}$ the set of twins with minimal average ([2], p. 15).

The sets T, $T_1 - T_4$ and S below will be supposed to be infinite.

In this paper some properties of Eratosthenes progression such as distribution laws of the progression elements, ζ–functions for the progressions and their connection with the Riemann ζ–function are only mentioned.

MESM

1
2 1
3 2 1
~~4~~
5 3 2 1
~~6~~
7 ~~4~~
~~8~~
~~9~~
~~10~~
11 5 3 2 1
~~12~~
13 ~~6~~
~~14~~
~~15~~
~~16~~
17 7 ~~4~~
~~18~~
19 ~~8~~
~~20~~
~~21~~
~~22~~
23 ~~9~~
~~24~~
~~25~~
~~26~~
~~27~~
~~28~~
29 ~~10~~
~~30~~
31 11 5 3 2 1
~~32~~
~~33~~
~~34~~
~~35~~
~~36~~
37 ~~12~~
~~38~~
~~39~~
~~40~~
41 13 ~~6~~
~~42~~
43 ~~14~~
~~44~~
~~45~~
~~46~~
47 ~~15~~
~~48~~
~~49~~
~~50~~
~~51~~
~~52~~
53 ~~16~~
~~54~~
~~55~~
~~56~~
~~57~~
~~58~~
59 17 7 ~~4~~
~~60~~
61 ~~18~~
~~62~~
~~63~~
~~64~~
~~65~~
~~66~~
67 19 ~~8~~
~~68~~
~~69~~
~~70~~
71 ~~20~~
~~72~~
73 ~~21~~
~~74~~
~~75~~
~~76~~
~~77~~
~~78~~
79 ~~22~~
~~80~~
~~81~~
~~82~~
83 23 ~~9~~
~~84~~
~~85~~
~~86~~
~~87~~
~~88~~
89 ~~24~~
~~90~~
~~91~~
~~92~~
~~93~~
~~94~~
~~95~~
~~96~~
97 ~~25~~
~~98~~
~~99~~
~~100~~
101 ~~26~~
~~102~~
103 ~~27~~
~~104~~
~~105~~
~~106~~
107 ~~28~~
~~108~~
109 29 ~~10~~
~~110~~
~~111~~
~~112~~
113 ~~30~~
~~114~~
~~115~~
~~116~~
~~117~~
~~118~~
~~119~~
~~120~~
~~121~~
~~122~~
~~123~~
~~124~~
~~125~~
~~126~~
127 31 11 5 3 2 1
~~128~~

Multiple Eratosthenes Sieve Machine

Figure 1:

The main result of this paper consists in the proposed plane–spiral geometric concept of arithmetic, compatible with the linear Cartesian concept.

The real semiaxis $\mathbb{R}^1_+$ in the new geometric model is isometrically mapped as *a logarithmic spline-spiral* on the plane $\mathbb{R}^2$ in such a way that the Eratosthenes rays, not intersecting each other, cross the spiral only at the primes.

The spiral arithmetic allows one to interpret in a new way the basic counting function $\pi(x)$, the Littlwood's Ω–theorem and also gives an arithmetic interpretation of the distribution in natural series of all kinds of clusters of primes (see [6], for example) and twin pairs, in particular.

The basic object in the spiral geometry is a *spider–web* W_n composed of spiral and Eratosthenes rays intersecting it, in which the number of rotations n infinitely increases.

The web W_n consists of embedded *concave–convex trapezoids* of primes with a characteristic formation law. This law is a direct consequence of the inner prime number distribution law.

The plane $\mathbb{R}^2$ is considered as *a mosaic* composed of *elementary concave–convex trapezoids.*

The web W_n *geometrically select (personalyzes)* primes, and also all kinds of linear and plane configurations of primes.

2 Splitting theorem for infinite sequences of primes

2.1 Basic definitions

Let sets $A \subset \mathbb{N}$ and $B \subset \mathbb{N}$ with the properties

$$A \cap B = \varnothing, \tag{1}$$

$$A \cup \overline{B} = \mathbb{N}, \tag{2}$$

where $\overline{B} = \{1\} \cup B$ are given.

Let the arithmetic function

$$g(n) : \mathbb{N} \to A$$

generate (denote) the nth element $a(n) \in A$.

Then the *counting recurrent law*

$$\varepsilon^+_{a(0)} : a(n+1) = g(a(n)),\ n = 0, 1, 2, \ldots, a(0) \in \mathbb{N} \tag{3}$$

determines *an A–counting progression* $\varepsilon^+_{a(0)}$ and *an A–counting ray*

$$r_{a(0)} = \{a(n) : a(n+1) = g(a(n)),\, n = 0, 1, 2, \ldots, a(0) \in \mathbb{N}\}.$$

Together with the function $g(n)$, its inverse function, the *nth number of element* $a(n) \in A$, is also uniquely determined (in a purely arithmetical sense it is a counting function)

$$g_{-1}(a) : A \to \mathbb{N}.$$

The functions $g(n)$ and $g_{-1}(a)$ are strictly monotonic and satisfy the equalities

$$g(g_{-1}(a)) = a, \quad g_{-1}(g(n)) = n.$$

By means of $g(n)$ and $g_{-1}(a)$ the compositions

$$g_n(a(0)) = \underbrace{g(\ldots g}_{n}(a(0))\ldots) = a(n),$$

$$g_{-n}(a(n_1)) = \underbrace{g_{-1}(\ldots g_{-1}}_{n}(a(n_1))\ldots), \quad \text{with } n \leq n_1.$$

are introduced.

These compositions satisfy the equalities

$$g_{n_1}(g_{n_2}(a(0))) = g_{n_1+n_2}(a(0)), \quad n_1, n_2 \geq 1,$$

$$g_{-n_1}(g_{n_2}(a(0))) = g_{n_2-n_1}(a(0)), \quad 1 \leq n_1 \leq n_2.$$

An extension of the A–counting progression $\varepsilon^+_{a(0)}$ with negative numbers $\varepsilon^-_{a(0)} = -\varepsilon^+_{a(0)}$ leads to an infinite cyclic group

$$\varepsilon_{a(0)} = \varepsilon^-_{a(0)} \cup \{a(0)\} \cup \varepsilon^+_{a(0)}, \quad g_{-n}(a(0)) = -g_n(a(0)),\ n > 0 \tag{4}$$

under composition $g_n(a(0))$, with *a depth* $n \in \mathbb{Z}$ and a *generator* $a(0) \in \overline{B}$.

Two elements from $\varepsilon_{a(0)}$ interact under the composition rule

$$g_{n_1}(a(0)) \circ g_{n_2}(a(0)) = g_{n_1}(g_{n_2}(a(0))) = g_{n_1+n_2}(a(0)),\ n_1, n_2 \in \mathbb{Z}. \tag{5}$$

2.2 Basic assertion and its consequences

The following assertion about the splitting of the set A in a denumerable number of denumerable subsets with a common law(3) of formation of its elements is given:

Theorem 1. *For any sets A and B with properties (1) and (2) the following equalities hold*

$$\bigcap_{a(0)\in\overline{B}} r_{a(0)} = \varnothing, \qquad \bigcup_{a(0)\in\overline{B}} r_{a(0)} = A\ .$$

Theorem 1 leads to a matrix representation of the sequences A and $\mathbb{N}$ with peculiar properties of their elements.

Corollary 1. *There exists an one-to-one mapping*

$$\overline{\varphi}(a(0)) : \overline{B} \to \ {}^2A = \{r_{a(0)}\}_{a(0)\in\overline{B}} \equiv \{a_{\mu\nu}\}_{\mu,\nu=1,2,\ldots} \tag{6}$$

(${}^2A$ denotes the matrix representation of the elements of A).

From (6) a matrix representation to the natural series

$${}^2\mathbb{N} = \|\overline{B} \quad {}^2A\|, \tag{7}$$

where $\overline{B} = \text{Column}\{a_{\mu 0}\}_{\mu=1,2,\ldots}$ also follows.

The matrices ${}^2A$ and ${}^2\mathbb{N}$ shall be called *mesm*–matrices.

In the case when $A = P$ and $B = M$ an example of the left upper corner of the matrix ${}^2\mathbb{N}$ ([2], pp. 18–22) is given in Appendix 1.

Corollary 2. *The rows of matrices ${}^2\mathbb{N}$ are isomorphic to the row r_1 with respect to the mapping*

$$\Psi(g_n(1)) : g_n(1) \to g_{-n}(g_n(1)) \to a(0) \to g_n(a(0)), \quad a(0) \in \overline{B}, \quad a(0) > 1.$$

The columns of the matrix ${}^2A$ are isomorphic to the column $\overline{B}$ with respect to the mapping

$$\varphi(a(0)) : a(0) \to g_n(a(0)), \quad a(0) \in \overline{B}.$$

In the case $A = P$ and $B = M$ Figure 2 illustrates mentioned isomorphisms. In Figure 2, an one-to-one correspondence between *rooted trees* and elements of $\mathbb{N}$, proposed by F. Göbel [7] is used (see the $1th$ row of Figure 2).

Theorem 1 leads also to an important consequence, which reveals the arithmetic nature of the fine structure of the set A elements' distribution among the natural numbers.

Let $g_{-1}(n', n'')$, $n', n'' \in \mathbb{N}$ denote the number of elements A in the interval (n', n'').

Corollary 3. *For the matrix* $[\overline{B}\ ^2A]$ *elements the following equalities hold:*

$$\left.\begin{aligned} &g_{-1}(a_{\mu 0}, 0) = a_{\mu_1} - 1, \quad \mu = 1, 2, \ldots, \\ &g_{-1}(a_{\mu_1\nu_1}, a_{\mu_2\nu_2}) = |a_{\mu_1(\nu_1-1)} - a_{\mu_2(\nu_2-1)}| - 1, \\ &\mu_i, \nu_i \geq 1, \quad i = 1, 2. \end{aligned}\right\} \tag{8}$$

3 The Theorem 1 application to special cases of sets A and B

3.1 About new A–counting progressions

In the case when A and B take usual values the law (3) generates known A–counting progressions. So, for example, at $A = \{even\}$ and $B = \{odd\}$ a generating function is of kind $g(a(n)) = 2a(n) - 1$ and in this case $\varepsilon_2^+ = \{2, 3, 5, 9, 17, 33, 65, 129 \ldots\}$ is a *Pisot sequence* ([4], A000051).

New A–progressions one occur when the behaviour of A elements among natural numbers is unknown and it cannot be considered as a probabilistic. Besides the sequences of primes P, all subsequences of P, in the formation of which the Eratosthenes sieve combines with an additional deterministic filter $f(n)$ (this is the formation rule of the considered subsequence), should also be considered belonging to this class. The set of these subsequences shall be denoted by $\mathcal{E}_f$.

The Dirichlet theorem about the existence of infinite primes of the kind $\alpha n + \beta$ (an additional filter) for arbitrary coprimes α and β shows that $\mathcal{E}_f$ is infinite.

In particular, we have inclusions $T_1, T_2, T_3, S \in \mathcal{E}_f$ *and* $D_{\alpha n \pm 1} \in \mathcal{E}_f$ *at* $\alpha = 4, 6$.

For all elements $\mathcal{E}_f$ there exists a *mesm*$_f$–process, which is analogous to the process represented in Figure 1. From the A–split theorem it follows that for every $A_f \in \mathcal{E}_f$ and $B_f = \mathbb{N} \setminus A_f$ there exists a *mesm*$_f$–matrix $[B_f\ {}^2A_f]$.

As a result of a *mesm*–transition $A_f \to\ {}^2A_f$, the elements of the rows ${}^2P$, ${}^2T_1$, ${}^2T_2$, ${}^2T_3$, ${}^2S$ and ${}^2D_{\alpha n \pm 1}(\alpha = 4, 6)$ already will be distributed according to the *inner law* (3), which now should be understood as a specific *self-smoothing* (only with respect to the rows ${}^2A_f$) of the irregularities in the appearance of the elements A_f in the natural series.

3.2 The basic case: $\mathbf{A = P}$ and $\mathbf{B = M}$.

The upper left corner of the matrix ${}^2P$ and its extension to the matrix ${}^2\mathbb{N}$ are represented in Appendix 1. The Theorem 1 has been proved inductively in [2], pp. 4–8.

The first elements of the first rows of the matrix ${}^2P$ were primarily determined *by hand* by means of *MESM* (Figure 1). In such a way the law (3) with $g(n) = p(n)$ (*Eratosthenes progressions*) was discovered [1].

The extension of the matrix ${}^2P$ rows on negative primes according to the rules (4), (5) leads to infinite cyclic groups under composition $p_n(a(0))$, $n \in \mathbb{Z}$ with a generators $a(0) \in M$. An example of such a group is the set

$$\varepsilon_4 = \{\ldots, -p_n(4), \ldots, -59, -17, -7, 4, 7, 17, 59, \ldots, p_n(4), \ldots\}.$$

A part of ${}^2P$ represented in Appendix 1 has been computed by means of **Mathematica** function **NestList[Prime, a(0), n]**.

The row elements of the matrix $[\overline{M}\ \ {}^2P]$ determine new subsets of natural numbers

$$N_m = \{p_{n_1}^{\alpha_1}(m) \ldots p_{n_k}^{\alpha_k}(m) : \forall\, n_i, \alpha_i \in \mathbb{N},\ i = 1, 2, \ldots, k,\ \forall\, k \in \mathbb{N}\},\ m \in \overline{M} :$$

$$N_1 = \{2, 3, 2^2, 5, 2 \cdot 3, 2^3, 3^2, 2 \cdot 5, 11, 2^2 \cdot 3, 3 \cdot 5, 2^4, \ldots\},$$

$$N_4 = \{7, 17, 7^2, 59, 7 \cdot 17, 277, 17^2, 7^3, 7 \cdot 59, 7^2 \cdot 17, 1787, 7^4, \ldots\},$$

$$N_6 = \{13, 41, 13^2, 179, 13 \cdot 41, 1063, 41^2, 13^3, 13^2 \cdot 41, \ldots\},$$

and so on.

According to Corollary 2, the behaviour of composite numbers reflects on the behaviour of the elements of the columns of the matrix ${}^2P$.

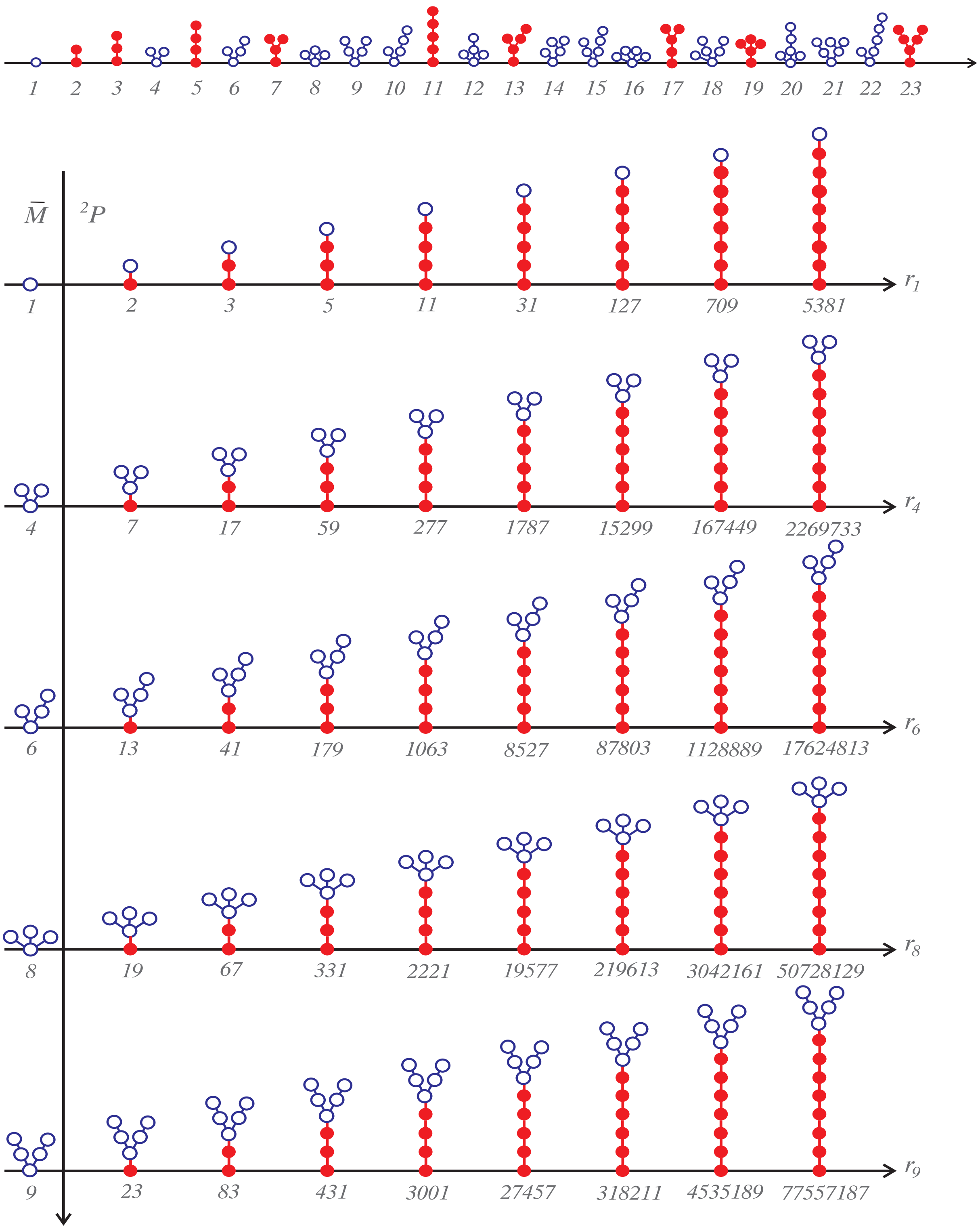

Figure 2: *"MESM & F. Göbel" forest of rooted trees*

On the other hand, the structure of the set M depends on the structure of the set of primes because M can be represented as a chain of α_μ–element segments (where $\alpha_\mu = d(\mu) - 1$) from consequent composite numbers

$$\overline{m}_\mu(\alpha_\mu) = \{p(\mu)+1, p(\mu)+2, \ldots, p(\mu+1)-1\}, \quad \mu = 2, 3, \ldots$$

$$(\overline{m}_2(1) = \{4\}, \overline{m}_3(1) = \{6\}, \overline{m}_4(3) = \{8, 9, 10\}, \ldots).$$

The segments are connected in a whole set M by means of *ghost primes* $\omega_\mu = \langle p(\mu) \rangle \quad (\omega_2 = \langle 3 \rangle, \omega_3 = \langle 5 \rangle, \omega_4 = \langle 7 \rangle, \ldots)$.

The Eratosthenes progressions $\{\varepsilon_m^+\}_{m \in \overline{M}}$ (i.e., rows of the matrix ${}^2P$) conform to the inner prime number distribution law

$$a(n+1) = p(a(n)) = p_{n+1}(a(0)), \quad n = 0, 1, 2, \ldots, a(0) \equiv m \in \overline{M}, \qquad (9)$$

but the deviation of the rows ${}^2P$ between each other (i.e., the distribution of primes in the columns of ${}^2P$) again persists dependent of the oddish behaviour of primes.

The main information left out of the inner law (9) is reflected in the structure of the first matrix ${}^2P$ column

$$P_1 = column[p_{11}, p_{21}, \ldots, p_{\mu 1}, \ldots].$$

The following assertion about the P_1 structure is valid.

Theorem 2. *Mapping $\varphi : a(0) \rightarrow p_{\mu 1}$ defines a correspondence between segments of composite numbers $\overline{m}_\mu(\alpha_\mu)$ and clusters of α_μ–successive primes*

$$c_\mu(\alpha_\mu) = \{p_1(p(\mu)+1), p_1(p(\mu)+2), \ldots, p_1(p(\mu+1)-1)\} \subset P$$

in the cases $\alpha_\mu \geq 3$, and separate primes $p_1(p(\mu)+1)$ in the cases $\alpha_\mu = 1$. At their ends the clusters are complemented by the ghost images up to prime number segments

$$\overline{c}_\mu(\alpha_\mu) = \{p_1(\langle p(\mu) \rangle), c_\mu(\alpha_\mu), p_1(\langle p(\mu+1) \rangle)\}$$

and the equality $P = \bigcup_{\mu=1}^{\infty} \overline{c}_\mu(\alpha_\mu)$ is fulfilled.

The next theorem about twin pairs $t(\nu) = (t_1(\nu), t_2(\nu)) \in T, \quad \nu = 3, 5, 7, \ldots$ is also justified.

Theorem 3. *For each pair $t(\nu)$(after the pair (3,5)) at least one of the elements $t_1(\nu)$ or $t_2(\nu)$ belongs to the first column P_1 .*

The mapping $\varphi^{-1}: p_{\mu 1} \to m_\mu$ defines a correspondence between pairs with both elements on P_1 (u–twin) and pairs of subsequent elements of some segment $\overline{m}_{\overline{\mu}}(\alpha_{\overline{\mu}}) \subset M$ with $\alpha_{\overline{\mu}} \geq 3$.

For a pair with one element $t_1(\nu)$ (or $t_2(\nu)$) on P_1 (b–twin) the mapping $\varphi^{-1}: p_{\mu 1} \to m(\mu)$ associates $t_1(\nu)$ (or $t_2(\nu)$) with the element $p(n)+1$, or the element $p(n+1)-1$ of some segment $\overline{m}_{\overline{\mu}}(\alpha_{\overline{\mu}}) \subset M$ at $\alpha_{\overline{\mu}} \geq 3$, or with the element of some one-element segment $\overline{m}_{\overline{\mu}}(1) \subset M$.

The mapping $\varphi^{-1}: p_{\mu_1 \nu_1} \to p_{\mu_1(\nu_1-1)}$, $\nu_1 \geq 2$ relates the second element $t_2(\nu)$ (or $t_1(\nu)$) to one of the ghosts $\langle p(\mu)\rangle \equiv p_{\mu_1(\nu_1-1)}$ or $\langle p(\mu+1)\rangle \equiv p_{\mu_1(\nu_1-1)}$.

The following properties of the matrix ${}^2P$ rows and columns are briefly veiwed:

q₁) The difference $d_m(n) = p_{(n+1)}(m) - p_n(m), \quad n = 1, 2, \ldots, m \in \overline{M}$ monotonically increase under the estimate

$$d_m(n) > p_n(m)(\ln p_n(m) - 1)$$

unlike the difference $d(n)$ whose behaviour only on the face of it may seems to be a chaotical one [8];

q₂) The sequence $\eta(s, m) = \sum\limits_{n=1}^{\infty} \frac{1}{p_n^s(m)}$ converge for all $m \in \overline{M}$ and $s \geq 1$.

Note especially the convergence of the sum $\eta(1, m)$ ([2], p. 10) when the sum $\sum\limits_{n=1}^{\infty} \frac{1}{p(n)}$ diverges;

q₃) An analogue of the Euler identity exists

$$\zeta(s, m)) \equiv 1 + \sum_{n \in N_m} \frac{1}{n^s} = \prod_{n=1}^{\infty} \left(1 - \frac{1}{p_n^s(m)}\right)^{-1}, \; m \in \overline{M}, s \geq 1;$$

$\mathbf{q_4}$) The Riemann function $\zeta(s) = \sum\limits_{n=1}^{\infty} \frac{1}{n^s}, \quad s \in \not{C}$ can be represented by the functions $\zeta(s,\, m)$

$$\zeta(s) = \prod_{m\in\overline{M}} \zeta(s,\, m);$$

$\mathbf{q_5}$) The asymptotic law for the primes and the simplified Riemann formula for $\pi(x)$ give an opportunity to find approximately $p_{n+1}(m)$, $m \in \overline{M}$ by solving the equations with respect to x

$$L(x) = p_n(m), \tag{10}$$

$$R(x) = p_n(m), \tag{11}$$

$$\text{where } L(x) = \int\limits_0^x \frac{ds}{\ln(s)},\ R(x) = \sum_{k=1}^{\infty} \frac{\mu(k)}{k} L(x^{1/k})$$

and $\mu(k)$ is a Möbius function;

$\mathbf{q_6}$) There exists an approximate formula

$$n = \int\limits_{\alpha}^{p_n(\beta)} \frac{ds}{s \ln\ln s} + \varepsilon(n,\, \beta), \tag{12}$$

where $\alpha = 11,\ \beta = 1,\ n > 4$ for $r_1,\ \alpha = 7,\ \beta = 4$ for r_4 and $\alpha = \beta = m$ for the other rays r_m.

The absolute error $|\varepsilon|$ for the part of the matrix $[\overline{M}\ \ {}^2P]$ in Appendix 1 is not greater than 0.2 when n is small and 0.06 when n is large.

Formula (12) is a *prime number distribution law* of the rays ${}^2P$.

On Figure 3, the behaviour of the function (12) is presented for the ray r_9;

$\mathbf{q_7}$) It is obvious that for the number μ of the element $p_{\mu n}$ in the matrix ${}^2P$ column

$$P_n = colomn[p_{1n}, p_{2n}, \ldots, p_{\mu n}, \ldots]$$

there exists an asymptotic formula

$$\mu \sim m - \int\limits_2^m \frac{ds}{\ln s}. \tag{13}$$

This is the column ${}^{2}P$ *prime number distribution law.*

In order to use (12) and (13) it is necessary to know the composite number m.

3.3 About other A–counting progressions

Applying the A–split theorem in the cases

$$A = T_1 \text{ and } B_1 = T_2 \cup M,$$

$$A = S \text{ and } B_2 = M \cup T_3,$$

$$A = D_{6n-1} \text{ and } B_3 = M \cup D_{6n+1} \cup \{2,3\},$$

and

$$A = D_{6n+1},\ B_4 = M \cup D_{6n-1} \cup \{2,3\},$$

we can obtain the next *mesm*-matrices of kind (7):

$$[B_1\,{}^{2}T_1] = \begin{bmatrix} 1 & 3 & 11 & 137 & 5639 & 641129 & 152921807\ldots \\ 2 & 5 & 29 & 641 & 44381 & 7212059 & \ldots \\ 4 & 17 & 239 & 12161 & 1583927 & \ldots & \\ 6 & 41 & 1151 & 93251 & 16989317 & \ldots & \\ 7 & 59 & 1931 & 176021 & 35263691 & \ldots & \\ 8 & 71 & 2339 & 221201 & 45749309 & \ldots & \\ . & . & . & . & . & \ldots & \end{bmatrix};$$

$$[B_2\,{}^{2}S] = \begin{bmatrix} 1 & 2 & 23 & 263 & 2917 & 38639 & 603311 & 11093633\ldots \\ 3 & 37 & 397 & 4751 & 64403 & 1038629 & 19661749 & \ldots \\ 4 & 47 & 491 & 5897 & 81131 & 1328167 & 25467419 & \ldots \\ 5 & 53 & 557 & 6709 & 93287 & 1541191 & 29778547 & \ldots \\ . & . & . & . & . & . & . & \ldots \\ 22 & 257 & 2861 & 37799 & 589181 & 10821757 & 230452837 & \ldots \\ 24 & 277 & 3079 & 40823 & 640121 & 11807167 & 252480587 & \ldots \\ . & . & . & . & . & . & . & \ldots \end{bmatrix};$$

$$[B_3\,{}^{2}D_{6n-1}] = \begin{bmatrix} 1 & 5 & 29 & 263 & 3767 & 76253 & 2049263 & 69633521\ldots \\ 2 & 11 & 83 & 953 & 16223 & 381221 & 11579489 & \ldots \\ 3 & 17 & 137 & 1721 & 31883 & 795803 & 25434641 & \ldots \\ 4 & 23 & 197 & 2663 & 51803 & 1348961 & 44635001 & \ldots \\ 6 & 41 & 419 & 6329 & 135347 & 3808109 & 134441441 & \ldots \\ . & . & . & . & . & . & . & \ldots \end{bmatrix};$$

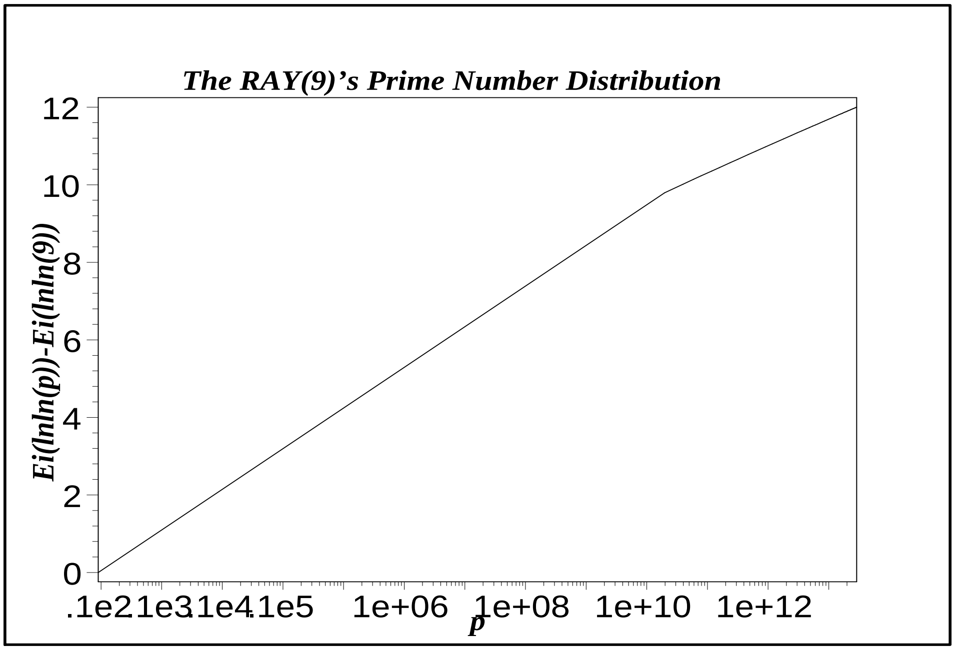

Figure 3:

$$[B_4\ {}^2D_{6n+1}] = \begin{bmatrix} 1 & 7 & 61 & 727 & 12343 & 284083 & 8457367 & 312953941\ldots \\ 2 & 13 & 109 & 1429 & 26113 & 642937 & 20262883 & 787318099\ldots \\ 3 & 19 & 181 & 2539 & 49669 & 1291471 & 42627997 & \ldots \\ 4 & 31 & 331 & 5011 & 105277 & 2908753 & 10144807 & \ldots \\ 5 & 37 & 397 & 6211 & 133633 & 3761239 & 132710947 & \ldots \\ \vdots & \vdots & \vdots & \vdots & \vdots & \vdots & \vdots & \ldots \end{bmatrix}.$$

The matrices $[B_1\ {}^2T_1]$, $[B_2\ {}^2S]$ and $[P\ \ {}^2M]$ were published in [4] as $A063502$, $A064110$ and $A025003$–$A025006$, respectively. Matrices $[B_3\ {}^2D_{6n-1}]$ and $[B_4\ {}^2D_{6n+1}]$ are the new ones.

New *mesm*–matrices can be obtained also for the Euler primes of the kind n^2+n+41 ($r_1 = \{41, 1847, 1573316, \ldots\}$), and for the Hardy-Littlwood primes of the kind $H_{n^2+1} = \{n^2+1 \in P : n = 1, 2, \ldots\}$ where at $B_5 = \mathbb{N} \setminus H_{n^2+1}$ we have

$$[B_5\ {}^2H_{n^2+1}] = \begin{bmatrix} 1 & 2 & 5 & 101 & 746497 & 286961228404901\ldots \\ 3 & 17 & 7057 & 11424189457\ldots & & \\ 4 & 37 & 44101 & 637723627777\ldots & & \\ 6 & 197 & 3496901\ldots & & & \\ 7 & 257 & 6421157\ldots & & & \\ \vdots & \vdots & \vdots & \vdots\ldots & & \end{bmatrix}.$$

All pointed out $mesm_f$–matrices are not studied. In particular, an analogue of the distribution laws (12) and (13) has not been found for them with the exception of the matrix $[P\ {}^2M]$ for which an analogue of the law (13) is known. However, the common Corollaries 2 and 3 of the A–split theorem remain valid for them.

4 Logarithmic geometry of primes on the plane.

4.1 The Prime Number Spider Web (PNSW) Hypothesis

One of the main application of *the prime number distribution law* (9) consists in constructing the plane spiral geometric concept of arithmetic.

Let

$$\mathfrak{L}_f = \{\rho(\theta) = (f(\theta))^{\theta} : \ f(\theta) \in C^1[0,\infty),\ f(\theta) \geq 1,\ 0 \leq \theta < \infty\}$$

denote a class of logarithmic spirals with an arc length

$$\lambda(0,\theta) = \int\limits_0^{\theta} (f(x))^x \left(\left(\ln f(x) + \frac{x f'(x)}{f(x)} \right)^2 + 1 \right)^{1/2} dx.$$

The plane spiral geometric concept is based on the following PNSW–hypothesis [1].

Conjecture 1. *On the plane* $\mathbb{R}^2$ *there exists a unique spiral* $\overline{\rho}(\theta) \in \mathfrak{L}_f$ *and the corresponding to it sets of angles*

$$\{\theta_{mn}\}_{m \in \overline{M}},\ n = 1,2,\ldots, \quad \theta_{mn'} < \theta_{mn''} \ \textit{at}\ n' < n''$$

such that the following conditions are fulfilled:

(i) $\lambda(0,\theta_{mn}) = p_n(m),\ n = 1,2,\ldots,\ m \in \overline{M}$;

(ii) the primes $p_n(m),\ n = 1,2,\ldots$ *lie on the same ray* $\ell_m \subset R^2$ *with a positive direction corresponding to increasing* n*;*

(iii) two arbitrary rays ℓ_{m_1} *and* ℓ_{m_2}*,* $m_1, m_2 \in \overline{M}$ *do not intersect each other and are non–parallel.*

4.2 Logarithmic spline–spiral

Under the substitution $f(\theta) = e^{\cot\varphi}$, $\mathfrak{L}_f$ turns in a one–parametric family of logarithmic spirals

$$\mathfrak{L}_\varphi = \left\{\rho_\varphi = e^{(\cot\varphi)\theta} : 0 < \varphi < \frac{\pi}{2},\, 0 \le \theta < \infty\right\}$$

with an arc length

$$\lambda(0,\theta) = \frac{1}{\cos\varphi}\left(e^{(\cot\varphi)\theta} - 1\right). \tag{14}$$

Now the required by the PNSW–hypothesis sets of angles with respect to m and n, according to the condition (i), are given by the formula

$$\theta_{mn} = \tan\varphi \ln(p_n(m)\cos\varphi + 1)).$$

For simple logarithmic spirals the conditions (ii) and (iii) of the PNSW–hypothesis are not fulfilled because the equation [1]

$$S_{n_1n_2}(x) + S_{n_2n_3}(x) + S_{n_3n_1}(x) = 0, \tag{15}$$

where

$$S_{\alpha\beta}(x) = (p_\alpha(m)x + 1)(p_\beta(m)x + 1)\sin\left(\sqrt{\frac{1}{x^2} - 1}\,\ln\frac{(p_\alpha(m)x + 1)}{(p_\beta(m)x + 1)}\right)$$

cannot be satisfied with the same value $x = \cos\varphi$ for any triplets $(p_{n_1}(m), p_{n_2}(m), p_{n_3}(m))$ from any ray r_m, $m \in \overline{M}$.

Nevertheless, the solution (15) for all the denoted prime triplets from all rays of the matrix in Appendix 1 shows that x remains in a sufficiently narrow interval $I_x = (0.202, 0.326)$ with an average $\overline{x} \approx 0.264$ to which there corresponds a value $\overline{\varphi} \approx 74.69°$. On Figure 4 a pure–logarithmic web is presented where only the condition (i) is fulfilled.

This result stimulates us to search for a verification of the PNSW–hypothesis in the class of logarithmic spline–spirals (LSS):

$$\rho_{s_1}(\theta) = e^{s_1(\theta)},$$

$$s_1(\theta) = \begin{cases} \alpha_{i+1}\theta + \beta_{i+1}, & \theta_i \le \theta \le \theta_{i+1} \quad 0 \le i \le k-1, \\ \alpha_{i-1}\theta_{i-1} + \beta_{i-1} = \alpha_i\theta_{i-1} + \beta_i, & 2 \le i \le k, \end{cases}$$

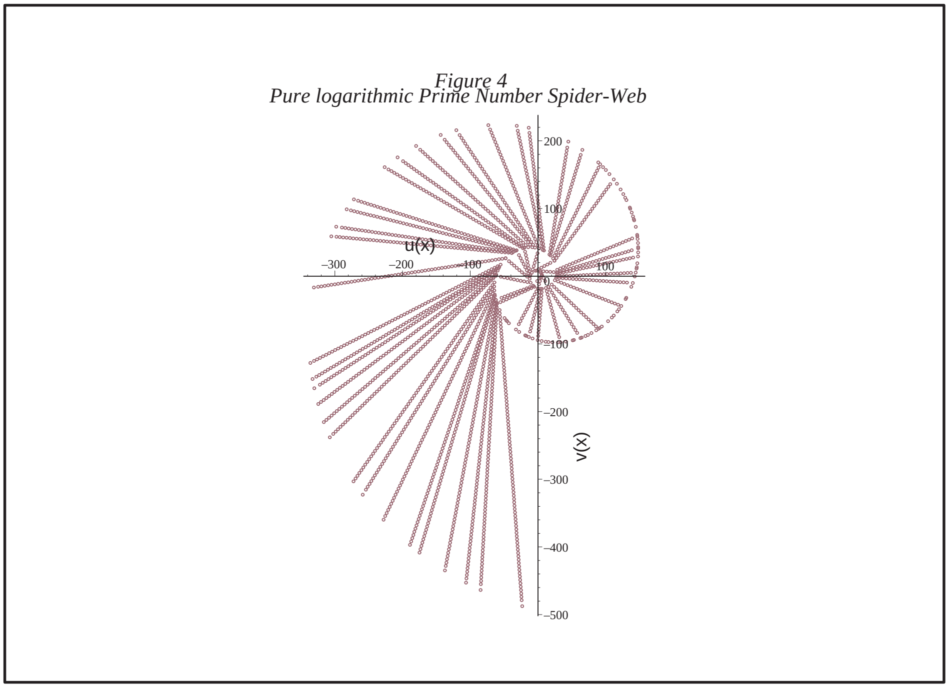

Figure 4: *Pure logarithmic prime number spider web*

where the first degree spline $s_1(\theta)$ is defined on an irregular set

$$\Delta_k : 0 = \theta_0 < \theta_1 < \theta_2 < \ldots < \theta_{k-1} < \theta_k,$$

with a number $k \geq 3$ of subintervals $[\theta_i, \theta_{i+1}], \quad 0 \leq i \leq k-1$, which increases with the number of rotations n of the web $W_n(P)$.

The unknowns in the spiral $\rho_{s_1}(\theta)$ are both the knots of the set Δ_k and the spline–spiral coefficients of the elements $e^{\alpha_i \theta + \beta_i}$

$$\{\alpha_i, \theta_i, \beta_i\}_{i=1,2,\ldots,k}.$$

They are determined from the conditions of the PNSW–hypothesis with regard for the initial condition

$$e^{\alpha_1 \theta_0 + \beta_1} = 1 \Longrightarrow \beta_1 = 0. \tag{16}$$

For arbitrary $x \in \mathbb{R}^1_+$ *there exists an unique* $p(k_x) \in P$ *such that* $p(k_x - 1) \leq x < p(k_x)$ *and the isometric transformation* $x \in \mathbb{R}^1_+$ *on* $\mathbb{R}^2$*, determined by the condition (i) of the PNSW–hypothesis, acquires the explicit form*

$$h_{\rho_{s_1}}(x) : \mathbb{R}^1_+ \to \lambda(0, \theta_x) = p(k_x - 1) + \sqrt{1 + \frac{1}{\alpha^2_{k_x}}}\ e^{\beta_{k_x}} \left(e^{\alpha_{k_x} \theta_x} - e^{\alpha_{k_x} \theta_{k_x - 1}} \right), \tag{17}$$

where

$$0 \le x < \infty, \quad \theta_x = \frac{1}{\alpha_{k_x}} \ln E(x),$$

$$E(x) = \frac{\alpha_{k_x}}{\sqrt{1+\alpha_{k_x}^2}} e^{-\beta_{k_x}}(x - p(k_x - 1)) + e^{\alpha_{k_x}\theta_{k_x-1}}, \quad p(0) = 0.$$

The points $(u_x, v_x) \in \rho_{s_1}(\theta) \subset \mathbb{R}^2$*, which correspond to the numbers* $x \in \mathbb{R}^1_+$*, have the Euler and Cartesian coordinates respectively:*

$$\rho(\theta_x) = e^{\alpha_{k_x}\theta_x + \beta_{k_x}} = e^{\beta_{k_x}} \ln E(x), \quad \theta_x = \frac{1}{\alpha_{k_x}} \ln E(x) \tag{18}$$

and

$$u_x = \rho(\theta_x)\cos(\theta_x), \quad v_x = \rho(\theta_x)\sin(\theta_x). \tag{19}$$

The first plane spiral isometric to the semi–axis $\mathbb{R}^1_+$ was constructed in [9].

4.3 About constructing the webs W_n

Attempts to construct the spiral $\rho_{s_1}(\theta)$ under the PNSW-hypothesis for a given n lead to a denial of some number k^0 of starting primes because of the difficulty in fulfilling the condition (ii) around the origin of $\mathbb{R}^2$ (condition (i) remains valid for the missed primes). In this paper the case $k^0 = 11$ is considered, i.e., instead of the rays r_1, r_4, r_6, r_8, r_9 and r_{10}, the truncated rays $\overline{r}_1, \overline{r}_4, \overline{r}_8, \overline{r}_9$ and $\overline{r}_{10}$ obey the condition (ii), and these rays start with the numbers $127, 59, 41, 87, 83$ and 109 respectively.

According to (16), to the first element $e^{\alpha_1\theta}$ $(0 \le \theta \le \theta_1)$ of the spiral ρ_{s_1} there corresponds the real segment $[0,\, p(k^0+1)]$.

The rotations W_n are taken in account from the ray

$$r_{12} = \{37, 157, 919, 7193, \dots\}$$

in the direction counter–clockwise.

At first, $\rho^{(3)}_{s_1}$ and W_3 are constructed on the basis of the first 3 elements of the first 25 rays $\overline{r}_1, \overline{r}_4, \dots, r_{36}$ plus the fourth element of the ray r_{12}.

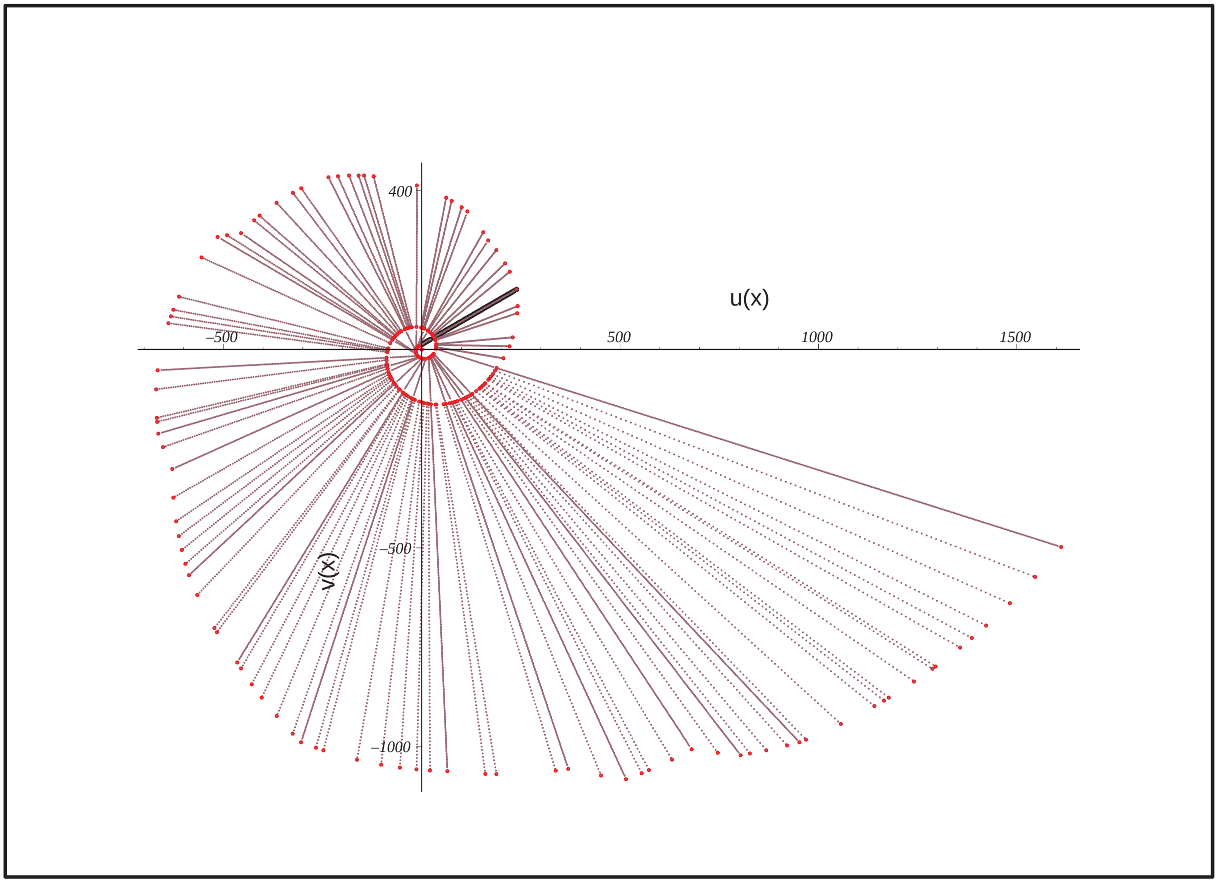

Figure 5: *3–rotation prime number spider web. The thick black line denotes the initial ray r_{12}. The direction of rotation is counter-clockwise*

The satisfaction of the conditions (i), (ii) of the PNSW–hypothesis with regard to (16) leads to a solution of a nonlinear system (W_3*–system*) of 228 equations and 304 inequalities, caused by the condition (iii), with respect to the 228 unknowns

$$\{\alpha_i, \theta_i, \beta_i\}_{i=1,2,\ldots,76} \ .$$

All 832 primes up to the number 7193, which remain unused in the construction of the W_3–system ($p_{-1}(7193) = 919;\ 11 + (25 \times 3 + 1) + 832 = 919$) are placed by the Cartesian coordinates (19) on the $2nd$ and $3rd$ rotation of $\rho^{(3)}_{s_1}$.

The building up of new rotations $n > 3$ on $\rho^{(3)}_{s_1}$ is reduced to the subsequent solution of 3×3 nonlinear systems of equations.

Both solvability and uniqueness of the mentioned infinite set of nonlinear systems are the analytical interpretation of the content of the PNSW-hypothesis.

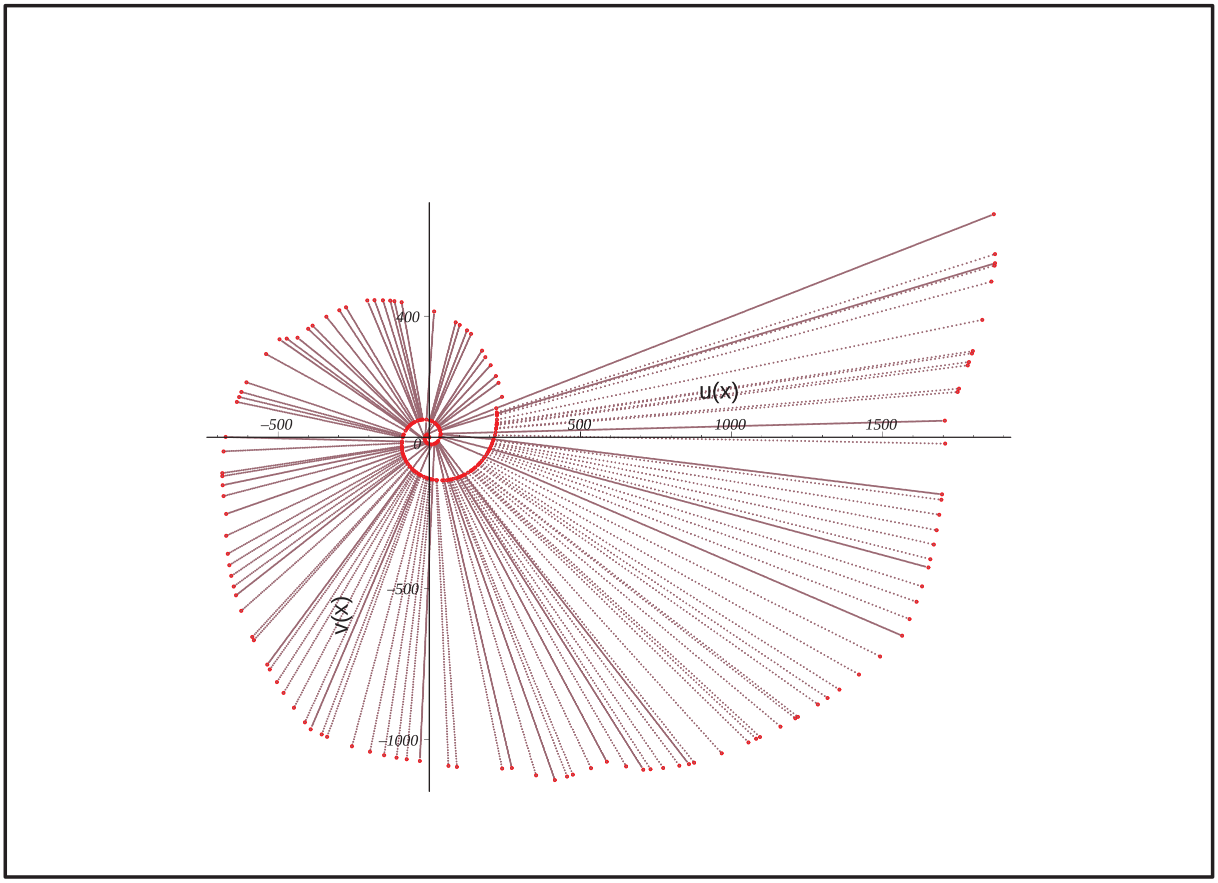

Figure 6: *3–rotation prime number spider web with full* 3*rd turn*

A desire to avoid the solution of the W_3–system leads to a construction of approximations $\widetilde{W}_3, \widetilde{W}_4$ and $\widehat{W}_3$, in which the first two turns are constructed as a simple spiral from $\mathfrak{L}_\varphi$. The subsequent rotations are constructed as LSS. In these webs $\varphi = 74.18896°$.

The web $\widetilde{W}_3$ fairly well illustrates the main properties of the prime number spider webs and the web $\widetilde{W}_4$ shows the possibility of continuing the construction of higher rotations. The web $\widehat{W}_3$ is created for a generation of initial approximations to a solution of the W_3–system. It also illustrates the demerits of the approximated webs.

The web $\widetilde{W}_3$ is presented in Figure 5. It is constructed on the basis of 211 primes: 3 numbers from each of the first 20 rays from $\overline{r}_1$ to r_{30}, 2 numbers from 5 rays from r_{32} to r_{36} and 2 numbers from each of the 71 rays from r_{38} to r_{126} $(3 \cdot 20 + 2 \cdot 5 + 2 \cdot 71 = 211)$; 147 of these primes are placed on the 2*nd* and the 3*rd* rotations by means of coordinates (19).

The web $\widetilde{W}_3$ does not have a complete 3*rd* rotation, ending in the number 5381 from the ray $\overline{r}_1$ and not reaching number 7193 from the initial

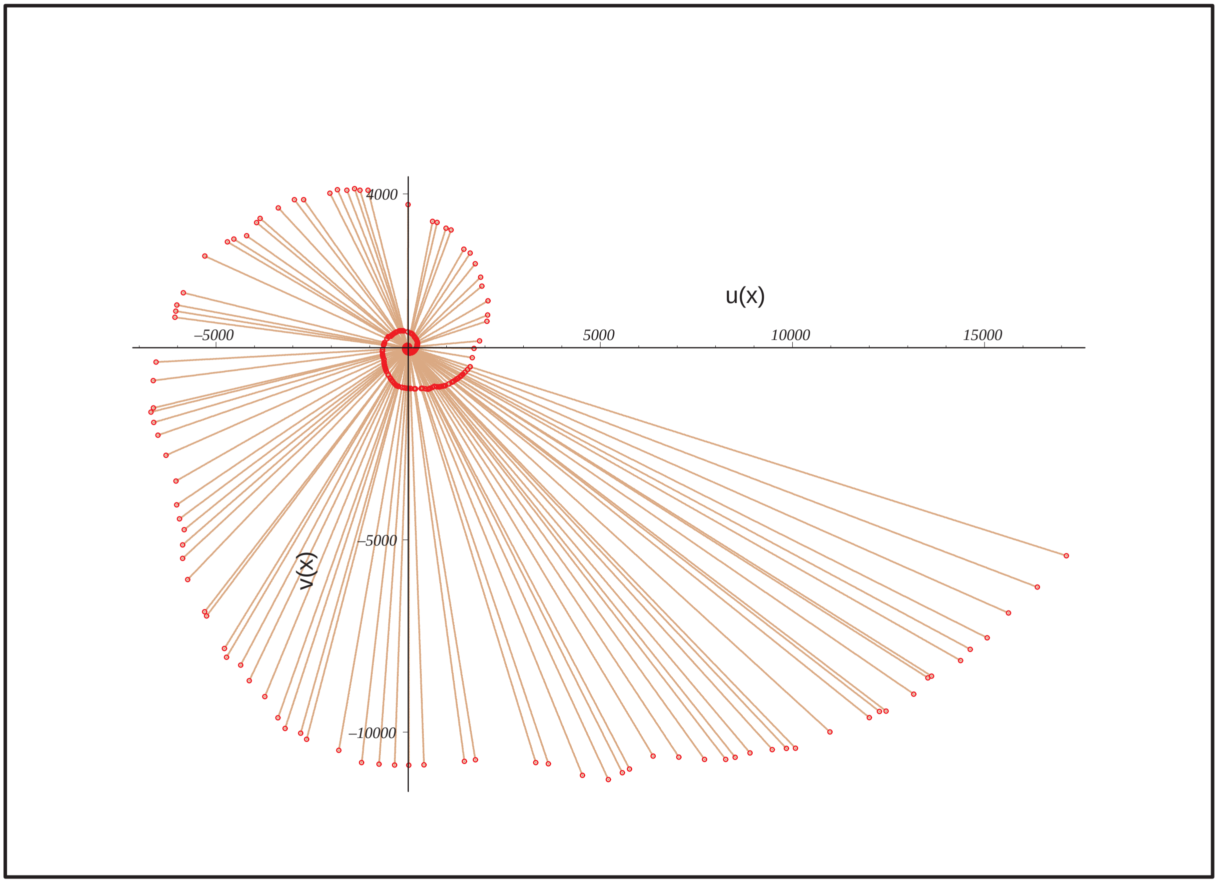

Figure 7: *4–rotation prime number spider web. In the center of the picture one can see the web* $\widetilde{W}_3$

ray r_{12}, marked in Figures 5 and 9 by a thick black line. To simplify the figure, 498 primes remaining until $p_{-1}(5381) = 709$ (709-211=498) are not placed on the $3rd$ rotation.

The web $\widehat{W}_3$ with a full $3rd$ rotation is represented in Figure 6. It is built on the basis of 255 primes: 3 from the first 25 rays from $\overline{r}_1$ to r_{36} and 2 from 90 rays from r_{38} to r_{151} $(3 \cdot 25 + 2 \cdot 90 = 255)$; 180 of these primes are placed on the $2nd$ and the $3rd$ rotations by means of coordinates (19).

To simplify the figure, 664 primes (919-255=664) remaining up to $p_{-1}(7193) = 919$ are not placed on the $3rd$ rotation.

At the end of the $3rd$ rotation $\widehat{W}_3$, (at the transition of the logarithmic spiral in LSS) a unessential *qualitative defect* shows up between numbers 877 from r_{36} and 919 from r_{12}. The pointed defect obstructs the exact sewing of the spirals between the numbers 6823 and 7193 from the corresponding rays r_{36} and r_{12}. This defect is removable by solving the W_3–system.

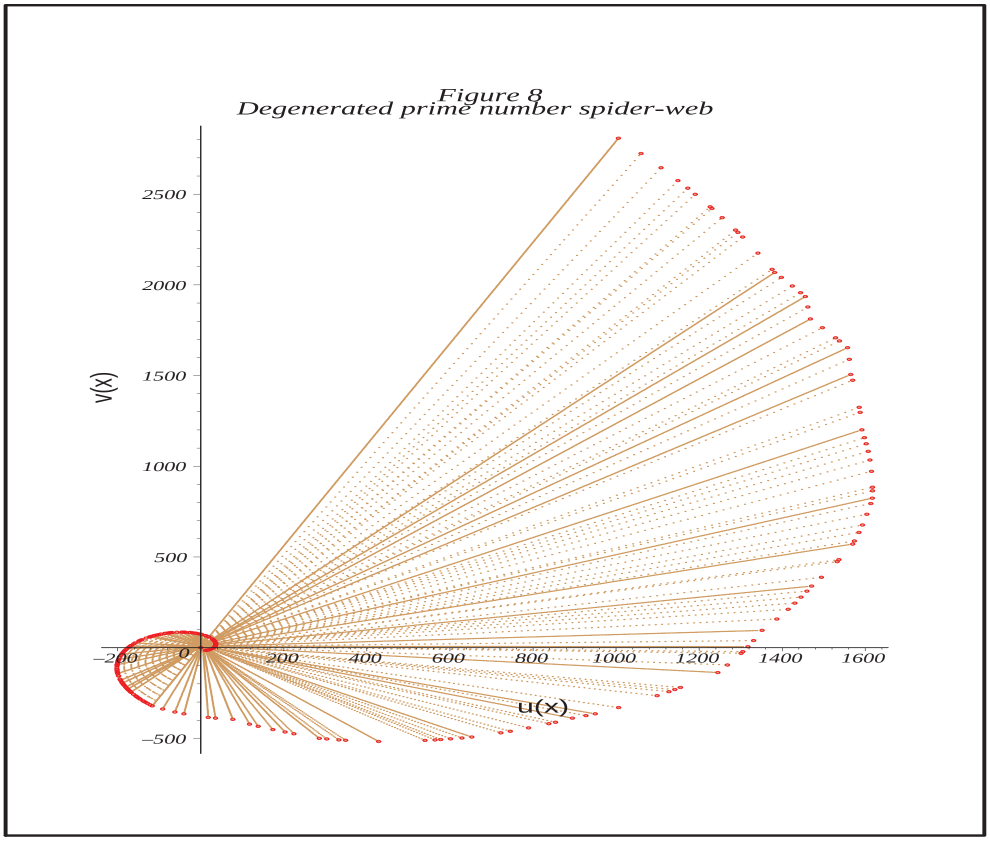

Figure 8: *Degenerated prime number spider web*

The web $\widetilde{W}_4$, represented in Figure 7, is obtained from the web $\widetilde{W}_3$ by adding on the $4th$ rotation as LSS. In this building, 96 primes are used: 4 elements of the rays from $\overline{r}_1$ to r_{30}, 3 elements of the rays from r_{32} to r_{36} and 4 elements of the rays from r_{38} to r_{126} (20+5+71=96). By means of 116 primes the LSS–units $e^{\alpha_i\theta_i + \beta_i}, \quad i = 1, 2, \ldots, 116$ are determined by solving a 3×3 nonlinear system 116 times with respect to 348 unknowns α_i, θ_i and β_i: 94 times exactly and 22 times approximately. The cases of inexact solutions result in unessential distortions of the condition (ii) for 22 rays (in the diagrams of $\widetilde{W}_3$ and $\widetilde{W}_4$ those distortions are not seen).

A variety of possibilities for constructing the PNSW–hypothesis is illustrated by web $\widetilde{W}_{deg}$ (Figure 8), in which the condition (ii) is violated in the following way: the rays lie on straight lines, but the subsequent segments of the rays have the opposite directions. In $\widetilde{W}_{deg}$, the same primes are used as in $\widetilde{W}_3$.

4.4 Web formation rules and properties

Satisfying the PNSW–hypothesis, the conditions of $\widetilde{W}_3$ and $\widetilde{W}_4$ fix the individual peculiarities of the behaviour of primes around the origin of $\mathbb{R}^2$ as concrete systems of embedded trapezoids confined between the rays $\ell_{p_{\mu 1}}$ and $\ell_{p_{(\mu+k)1}}$, $k \geq 1$. For example, the trapezoid t_{19} confined between the rays ℓ_{113} and ℓ_{127} (Figure 9) is one of the nineteen *3-rotation embedded trapezoids (3RET)* of the web $\widetilde{W}_3$.

From the Theorem 2 it follows that

q$_8$) The elements of the clusters $c_{\alpha_\mu}(\alpha_\mu)$ (they and only they) become the starts of new rays on the spiral $\rho_{s_1}(\theta)$.

Let a cluster

$$c_\mu(k) = \{p_{\mu 1}, p_{(\mu+1)1}, \ldots, p_{(\mu+k)1}\}.$$

lie on the νth rotation of the spiral $\rho_{s_1}^{(n)}(\theta)$. On the $(\nu+q)$th rotation to it there correspond the primes $\{p_q(p_{(\mu+i)1})\}_{i=0,1,\ldots,k}$.

The PNSW–hypothesis shows that

q$_9$) The geometric figure on $\mathbb{R}^2$, confined between the arcs $(p_{\mu 1}, p_{(\mu+k)1})$ and $(p_q(p_{\mu 1}), p_q(p_{(\mu+k)1}))$ by the spiral ρ_{s_1} and the segments $|p_{\mu 1}, p_q(p_{\mu 1})|$, $|p_{(\mu+k)1}, p_q(p_{\mu+k})|$ of the rays $\ell_{p_{\mu 1}}$ and $\ell_{p_{(\mu+k)1}}$, is the concave–convex trapezoid

$$z(\nu, \mu, k, q) = [(p_{\mu 1}, p_{(\mu+k)1}),\ (p_q(p_{\mu 1}), p_q(p_{(\mu+k)1}))].$$

The trapezoids of the type $z(\nu, \mu, 1, 1)$ are *elementary trapezoids (or holes)* to W_n. For example

$$z(1, 19, 1, 1) = [(113, 127), (617, 709)]$$

is an elementary W_2–trapezoid (Figure 10).

Let the primes $p_{\mu 1}$, $p_{(\mu+k)1} \in c_\mu(\alpha_\mu), \alpha_\mu \geq 3,\ 0 \leq k \leq \alpha_\mu$ lie on the νth rotation of the spiral $\rho_{s_1}^{(n)}$. On the $(\nu+1)$th rotation, to them there corresponds the cluster $c_{\mu_1}(\alpha_{\mu_1}) = \{p_{\mu_1 1}, p_{(\mu_1+1)1}, \ldots, p_{(\mu_1+\alpha_{\mu_1})1}\}$ with a length $\alpha_{\mu_1} = p_{(\mu+k)1} - p_{\mu 1} - 1$, according to Corollary 3.

From the conditions of the PNSW-hypothesis there stems the following rule for formation of 3RET:

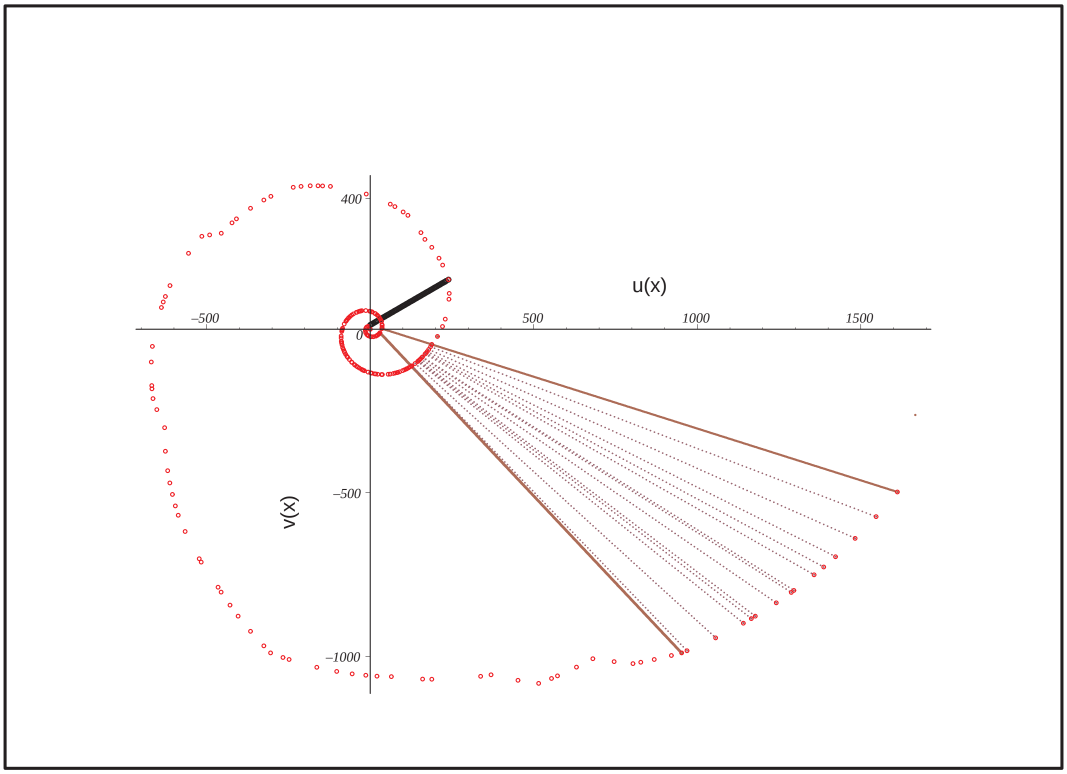

Figure 9: *3–rotation system of embedded trapezoids* $3RET_{19} = z(1, 19, 1, 2) = [(113, 127), (4549, 5381)]$*. The thick black line defines the initial ray* r_{12}*. The direction of rotation is counter-clockwise*

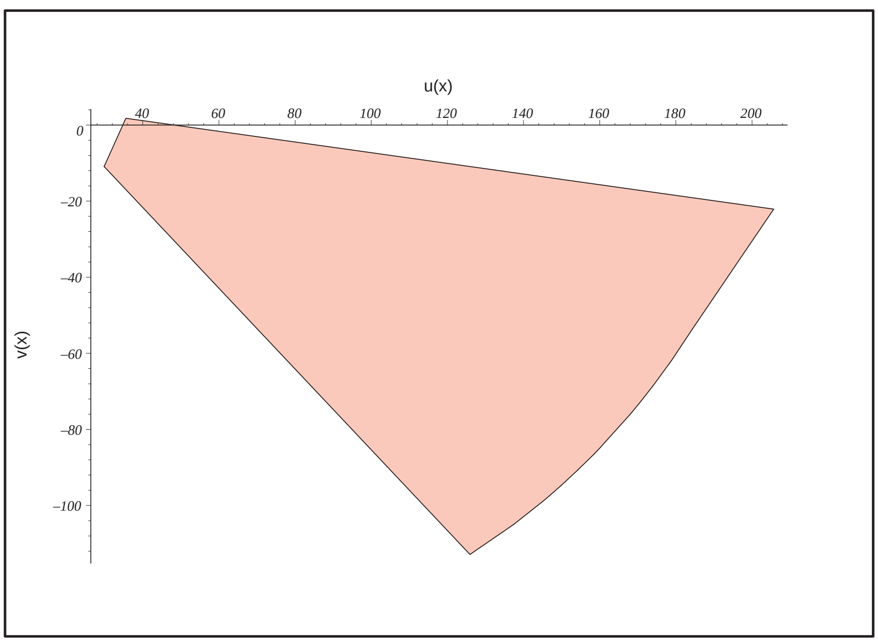

Figure 10: *The elementary trapezoid* $z_{19} = z(1, 19, 1, 1) = [(113, 127), (617, 709)]$

q$_{10}$) On the plane $\mathbb{R}^2$ the following equalities hold

$$z(\nu+1,\mu_1,\alpha_{\mu_1}+1,1)=\bigcup_{i=0}^{\alpha_{\mu_1}} z(\nu+1,\mu+i,1,1), \tag{20}$$

$$z(\nu,\mu,1,2)=z(\nu,\mu,1,1)\cup z(\nu+1,\mu_1,\alpha_{\mu_1}+1,1). \tag{21}$$

Equalities (20) and (21) can be regarded as those between the areas (the sign $\cup$ changes to $+$).

Let us apply the rule for formation of 3RET to $3RET_{19}$. Using the matrix from Appendix 1, we obtain

$$3RET_{19}=[(113,127),\,(617,709)]\cup[(617,619),\,(4549,4567)]\cup$$

$$[(619,631),\,(4567,4663)]\cup\ldots\cup[(701,709),\,(5281,5381)].$$

In this example $\nu=1$, $\mu=30$, $\alpha_{\mu_1}=127-113-1=13$. The starts of the newly–appeared rays on the second rotation are

$p(114)=619,\ \ p(115)=631,\ \ p(116)=641,\ \ p(117)=643,$
$p(118)=647,\ \ p(119)=653,\ \ p(120)=659,\ \ p(121)=661,$
$p(122)=673,\ \ p(123)=677,\ \ p(124)=683,\ \ p(125)=691,$ and
$p(126)=701.$

q$_{11}$) The rule for formation of 3RET shows that 3RET is a mosaic of $\alpha_{\mu_1}+1$ elementary trapezoids, which are grouped in the direction of the ray $\ell_{p_{\mu 1}}$ in the following way:
the first is the elementary trapezoid

$$[(p_{\mu 1},\,p_{(\mu+1)1}),\,(p_1(p_{\mu 1}),\,p_1(p_{(\mu+1)1}))],$$

followed by the composite trapezoid

$$[(p_1(p_{\mu 1}),\,p_1(p_{(\mu+\alpha_{\mu_1})1})),\,(p_2(p_{\mu 1}),\,p_2(p_{(\mu+\alpha_{\mu_1})1}))].$$

The elements (elementary trapezoids too) of the last one cause in total $\mu_2=p_1(p_{(\mu+\alpha_{\mu_1})1})-p_1(p_{\mu 1})-1$ new rays on the $(\nu+2)th$ rotation, to which again the 3RET formation rule is applied for obtaining α_{μ_2} new composite trapezoids located between the $3rd$ and $4th$ rotations of W_n.

Under the condition of the PNSW-hypothesis the process of growth of the initial 3RET is unlimited and leads to the formation of *a class* $(\ell_{p_{\mu 1}},\, \ell_{p_{(\mu+1)1}})$*–trapezoids* containing an unlimited number of different elementary trapezoids.

q_{12}) Let *mitos* denote a closed geometric figure locked between the arc $(p(12), p_1(12)))$ of the spiral ρ_{s_1} and the segment $|p(12), p_1(12)|$ of the ray r_{12}. Then the plane $\mathbb{R}^2$ can be represented as a mosaic of the initial $k(k^0)$–classes of embedded trapezoids (k(11)=25):

$$\mathbb{R}^2 = \bigcup_{i=1}^{k(k^0)} \left(\ell_{p(k^0+i)},\, \ell_{p(k^0+i+1)}\right) \cup mitos.$$

Inside the *mitos* the starts of the first few rays can intersect each other, i.e., be in a mitosis status.

Properties q_{10}), q_{11}) and q_{12}) are generalized in the property q_{13}.

q_{13}) The plane $\mathbb{R}^2$ is representable as a mosaic (in the theoretical–set sum sense) of all the prime–numerical elementary trapezoids and *mitos.*

q_{14}) The PNSW-hypothesis leads to the geometric interpretation of $\pi(x)$:

$$\pi(p_\nu(m)) = p_{\nu-1}(m) = \lambda(0,\, p_{\nu-1}(m)), \quad \nu \geq 2,\, m \in \overline{M}. \tag{22}$$

Equalities (22) allow one to interpret geometrically the Ω–theorem of Littlwood and Theorem 1 from [10], where for setting the real values and in particular the values of $Li(x)$ again the transformation $h_{\rho_{s_1}}(x)$ and coordinates (19) are used.

The geometric interpretation of the Theorem 3 consists in determination of the laws for appearance of u– and b–twins on W_n.

q_{15}) u–twins appear on W_n in the following cases:

a) as starts of new rays $\ell_{p_{\mu 1}}$ and $\ell_{p_{(\mu+1)1}}$ on the $1st$ rotation 3RET, which on the $2nd$ rotation cause one new ray $\ell_{p((p_{\mu 1}+p_{(\mu+1)1})/2)}$. Then 3RET is composed of three elementary trapezoids.

Examples:

$$\overline{m}_8(3) \to (\ell_{71}, \ell_{73}) \to \ell_{359},$$

$$\overline{m}_9(5) \to (\ell_{101}, \ell_{103}) \to \ell_{557},$$

$$\overline{m}_{11}(5) \rightarrow \begin{cases} (\ell_{137}, \ell_{139}) \rightarrow \ell_{787}, \\ (\ell_{149}, \ell_{151}) \rightarrow \ell_{863}; \end{cases}$$

b) as a pair of subsequent primes on the $2nd$ rotation of 3RET

Examples on the $2nd$ turn of the trapezoid $z(1, 19, 1, 2)$ (Figure 9):

$$\overline{m}_{30}(13) \rightarrow \begin{cases} (\ell_{641}, \ell_{643}) \rightarrow \ell_{4783}, \\ (\ell_{659}, \ell_{661}) \rightarrow \ell_{4937}. \end{cases}$$

$\mathbf{q_{16}}$) One of the elements of b–twin $(t_1(\overline{n}),\ t_2(\overline{n}))$ lies on the existing ray $\ell_{p_q(p_{\mu_1 1})},\ q \geq 1$, but the other element is a start of a new ray $\ell_{p_{\mu_2 1}}$:

$$t_1(\overline{n}) \equiv p_q(p_{\mu_1 1}),\ t_2(\overline{n}) \equiv p_{\mu_2 1} \text{ -- } right \text{ twin;}$$

$$t_1(\overline{n}) \equiv p_{\mu_2 1},\ t_2(\overline{n}) \equiv p_q(p_{\mu_1 1}) \text{ -- } left \text{ twin}$$

In such a way the b–elementary trapezoid

$$[(p_q(p_{\mu_1 1}), p_{\mu_2 1}),\ (p_{q+1}(p_{\mu_1 1}), p(p_{\mu_2 1}))]$$

is sewn together to the right of the ray $\ell_{p_{\mu_1 1}}$, and trapezoid

$$[(p_{\mu_2 1}, p_q(p_{\mu_1 1})),\ (p(p_{\mu_2 1}), p_{q+1}(p_{\mu_1 1}))]$$

to the left of the ray $\ell_{p_{\mu_1 1}}$.

Examples: the trapezoid $[(617, 619),\ (4549, 4567)]$ is sewn to the right of the ray ℓ_{113} $((\ell_{617}, \ell_{619}) \rightarrow \ell_{4561})$;

the trapezoid $[(857, 859),\ (6653, 6661)]$ is sewn to the left of the ray ℓ_{149} $((\ell_{857}, \ell_{859}) \rightarrow \ell_{6659})$.

The properties q_{15}) and q_{16}) show the following W_n sewing property

$\mathbf{q_{17}}$) The twin pairs *sew* uniformly over n the Eratosthenes rays in an *unified* plane web W_n, $n = 1, 2, \ldots$.

5 Conclusion

The study of the inner prime number distribution law remains at the initial stage.

Finally, we shall note how the proof of Conjecture 1 looks like, and we shall find a possibility of its generalization. We should like to indicate possible applications of the proposed, in this paper, approach to a study of the oddish prime number behaviour.

At the first stage of the proof of Conjecture 1 it is necessary to solve the W_3–system and revise the number k^0. If the W_3–system cannot be solved with $k^0 = 11$, then the numbers $k^0 = 10$ and $k^0 = 12$ should be tried.

In the formulation of the W_3–system a function $\tilde{p}(x) \in C^1(0, 10000]$, with a property

$$\tilde{p}(n) = p(n), \quad n = 1, 2, \ldots, 1229 \tag{23}$$

is used.

This function can be built up by *the rod spline method* [11] using as a rod the approximation ([12], exercise 9.21)

$$\overline{p}(x) = x\left(\ln x + \ln\ln x + \frac{\ln\ln x - 2}{\ln x} - \frac{(\ln\ln x)^2/2 - 3\ln\ln x + 5.5}{(\ln x)^2} - 1\right).$$

The searched function will be of the form $\tilde{p}(x) = s_2(x)\overline{p}(x)$, where $s_2(x)$ is a parabolic spline determined on two nonuniform sets. At the interpolation points equalities (23) are fulfilled.

The W_3–system solvability can first be investigated numerically by using, for example, the program LANCELOT [13].

At the second stage of the proof of Conjecture 1, it is necessary to prove inductively the continuability of the *basic* $k(k^0)$*–classes of embedded trapezoids*

$$(\ell_{p_{(k^0+i)1}}, \ell_{p_{(k^0+i+1)1}}), \quad i = 1, 2, \ldots, k(k^0),$$

as well as the continuability of *the new classes on rotations* $n \geq 2$.

Conjecture 1 can be extended to all $mesm_f$–matrices.

Conjecture 2. *For each matrix $A_f \in \mathcal{E}_f$ there exists LSS-spiral and a web $W_n(A_f)$, satisfying the conditions (i), (ii) and (iii) of the PNSW–hypothesis.*

In the infinite set of webs $\mathbf{w} = \{W_n(A_f) : A_f \in \mathcal{E}_f,\ n = 1, 2, \ldots\}$ it is necessary to introduce an operation *summing webs* @ in such a way that the equalities

$$W_n(S)@W_n(T_1)@W_n(T_2) = W_n(P)$$

and

$$W_n(D_{6n-1})@W_n(D_{6n+1}) = W_n(P),$$

hold, by analogy with the set-theoretical equalities $P = S \cup T_1 \cup T_2$ and $P = D_{6n-1} \cup D_{6n+1} \cup \{2, 3\}$, where$\{2, 3\} \subset$ *mitos*.

On the whole, the algebraic structures of mesm-matrices $[B_f\ {}^2A_f]$, webs $W_n(A_f)$ and the set $\mathbf{w}$ remain unexplored.

The spiral $\rho_{s_1}(\theta)$ length from the PNSW–hypothesis can turn out to be an appropriate *time coordinate* in the description of physical processes taking place in asymmetric and irreversible time.

Indeed, the mapping (17) can be extended also for negative values $x \in (-\infty, 0]$:

$$h\rho_{s_1}(x) : \mathbb{R}^1_- \to \lambda(0, \theta_x) = \frac{1}{\cos\varphi}\left(e^{(\cot\varphi)\theta_x} - 1\right),$$

$$-\infty < x \leq 0,\ \varphi = \operatorname{arccot}(\alpha_1).$$

In such a way, in the unit circle (inside the domain *mitos*) there remains a finite *negative moustache* with a length

$$\lambda(0, -\infty) = -\frac{1}{\cos\varphi}.$$

Now, the arc length of the spiral $\rho_{s_1}(\theta)$, $-\infty < \theta < \infty$ is split up in three pieces: the length of *the negative moustache*, the finite positive length spiral in the *mitosis* and the infinite arc length corresponding to the semi-axis $[p(k^0 + 1), \infty)$.

The solution of equations (10), (11) provides a motivation for the following hypothesis:

Conjecture 3. *For arbitrary $m \in \overline{M}$ and large n the inequality*

$$|L(p_{n+1}(m)) - p_n(m)| \leq c_1\sqrt{p_{n+1}(m)}\ln(p_{n+1}(m)) \tag{24}$$

is fulfilled with a constant c_1 independent of m .

Inequalities (24) result in the common estimate

$$|L(x) - \pi(x)| < c_2\sqrt{x}\ln x,\ c_2 = const. \tag{25}$$

The proof of inequality (24) is easier than the proof of inequality (25). If from estimation (25) follows the truth of the Riemann hypothesis that complex solutions of the equations $\zeta(s) = 0,\ s \in \mathbb{C}$ have a form $s = 1/2 + i\gamma_n,\ \gamma_n \in \mathbb{R},\ n = 1, 2, \ldots,$ then the inner prime number distribution law (9) will prove to be a new useful tool of the analytical number theory.

Appendix 1

Matrix [$\overline{\mathbf{M}}\ {}^{2}\mathbf{P}$]

1	2	3	5	11	31
		127	709	5381	52711
		648391	9737333	174440041	3657500101
		88362852307	2428095424619		
		75063692618249...			
4	7	17	59	277	1787
		15299	167449	2269733	37139213
		718064159	16123689073	414507281407	
		12055296811267...			
6	13	41	179	1063	8527
		87803	1128889	17624813	326851121
		7069067389	175650481151	4952019383323...	
8	19	67	331	2221	19577
		219613	3042161	50728129	997525853
		22742734291	592821132889	17461204521323...	
9	23	83	431	3001	27457
		318211	4535189	77557187	1559861749
		36294260117	963726515729	28871271685163...	
10	29	109	599	4397	42043
		506683	7474967	131807699	2724711961
		64988430769	1765037224331	53982894593057...	
12	37	157	919	7193	72727
		919913	14161729	259336153	5545806481
		136395369829	3809491708961...		
14	43	191	1153	9319	96797
		1254739	19734581	368345293	8012791231
		200147986693	5669795882633...		
15	47	211	1297	10631	112129
		1471343	23391799	440817757	9672485827
		243504973489	6947574946087...		
16	53	241	1523	12763	137077
		1828669	29499439	563167303	12501968177
		318083817907	9163611272327...		
18	61	283	1847	15823	173867
		2364361	38790341	751783477	16917026909
		435748987787	12695664159413...		
20	71	353	2381	21179	239489
		3338989	56011909	1107276647	25366202179
		664090238153	19638537755027...		
21	73	367	2477	22093	250751
		3509299	59053067	1170710369	26887732891
		705555301183	20909033866927...		

Appendix 1

Matrix [$\overline{\mathbf{M}}$ $^{2}\mathbf{P}$]. . . Continuation 1.

22	79	401	2749	24859	285191
		4030889	68425619	1367161723	31621854169
		835122557939	24894639811901...		
24	89	461	3259	30133	352007
		5054303	87019979	1760768239	41192432219
		1099216100167	33080040753131...		
25	97	509	3637	33967	401519
		5823667	101146501	2062666783	48596930311
		1305164025929	39510004035659...		
26	101	547	3943	37217	443419
		6478961	113256643	2323114841	55022031709
		1484830174901	45147154715447...		
27	103	563	4091	38833	464939
		6816631	119535373	2458721501	58379844161
		1579041544637	48112275898789...		
28	107	587	4273	40819	490643
		7220981	127065427	2621760397	62427213623
		1692866362237	51702420222709...		
30	113	617	4549	43651	527623
		7807321	138034009	2860139341	68363711327
		1860306318433	56997887937671...		
32	131	739	5623	55351	683873
		10311439	185350441	3898093877	94434956839
		2606906998739	80783250929599...		
33	137	773	5869	57943	718807
		10875143	196100297	4135824247	100450108949
		2773622459039	86127342906779...		
34	139	797	6113	60647	755387
		11469013	207460717	4387715993	106839327589
		2956887579073...			
35	149	859	6661	66851	839483
		12838937	233784751	4973864561	121763369327
		3386468161121...			
36	151	877	6823	68639	864013
		13243033	241568891	5147813641	126206581463
		3514741569337...			
38	163	967	7607	77431	985151
		15239333	280256489	6016014239	148471002899
		4159843299587...			

Appendix 1

Matrix $[\overline{\mathbf{M}}\ {}^{2}\mathbf{P}]$... Continuation 2.

39	167	991	7841	80071	1021271
		15837299	291905681	6278569691	155231019913
		4356423418499...			
40	173	1031	8221	84347	1080923
		16827557	311234591	6715304579	166500464477
		4684808232443...			
42	181	1087	8719	90023	1159901
		18143603	337033877	7300206493	181639026043
		5127173445557...			
44	193	1171	9461	98519	1278779
		20137253	376292689	8194134017	204869160779
		5808496248769...			
45	197	1201	9739	101701	1323503
		20890789	391182829	8534307629	213736527847
		6069307408303...			
46	199	1217	9859	103069	1342907
		21219089	397681327	8682977119	217616274683
		6183541562551...			
48	223	1409	11743	125113	1656649
		26548261	503859997	11126538823	281736685679
		8081022964981...			
49	227	1433	11953	127643	1693031
		27170047	516340703	11415461989	289357897711
		8307635814431...			
50	229	1447	12097	129229	1715761
		27560453	524172379	11596829689	294145810687
		8450108859131...			
51	233	1471	12301	131707	1751411
		28171007	536433767	11881126321	301656862553
		8673774992821...			
52	239	1499	12547	134597	1793237
		28889363	550881943	12216514841	310526940547
		8938160481557...			
54	251	1597	13469	145547	1950629
		31599859	605555557	13489097663	344268078839
		9946200971687...			
55	257	1621	13709	148439	1993039
		32332763	620393003	13835380799	353471438263
		10221768670013...			
56	263	1669	14177	153877	2071583
		33691309	647927381	14478972721	370600719481
		10735307868743...			

Appendix 1

Matrix [$\overline{\mathbf{M}}\ {}^{\mathbf{2}}\mathbf{P}$]... Continuation 3.

57	269	1723	14723	160483	2167937
		35368547	682005953	15277169617	391886115431
		11374585999793...			
58	271	1741	14867	162257	2193689
		35815873	691097513	15490445177	397580778799
		11545824668459...			
60	281	1823	15641	171697	2332537
		38235377	740436923	16649917331	428592846379
		12479807093519...			
62	293	1913	16519	182261	2487943
		40951019	796000427	17959785803	463728180431
		13540770614753...			
63	307	2027	17627	195677	2685911
		44432569	867503173	19651365719	509248998611
		14919411840803...			
64	311	2063	17987	200017	2750357
		45564719	890830471	20204583739	524169678691
		15372235794151...			
65	313	2081	18149	202001	2779781
		46082987	901517753	20458245581	531016168117
		15580165580489...			
66	317	2099	18311	204067	2810191
		46620709	912598217	20721384791	538121923037
		15796066509169...			
68	337	2269	20063	225503	3129913
		52286593	1029838717	23513901553	613739626127
		18099406558319...			
69	347	2341	20773	234293	3260657
		54615469	1078227191	24670634249	645165616243
		19059563752283...			
70	349	2351	20899	235891	3284657
		55043683	1087126459	24883634693	650958710863
		19236734782351...			
72	359	2417	21529	243781	3403457
		57160969	1131224411	25940205719	679722101701
		20117195040149...			
74	373	2549	22811	259657	3643579
		61460533	1221036307	28097383163	738585245417
		21922891272739...			
75	379	2609	23431	267439	3760921
		63567289	1265161649	29159843309	767640499331
		22816010162129...			

Appendix 1

Matrix [$\overline{\mathbf{M}}$ $^{\mathbf{2}}\mathbf{P}$]... Continuation 4.

76	383	2647	23801	271939	3829223
		64795981	1290918281	29780778613	784640376427
		23339094889519...			
77	389	2683	24107	275837	3888551
		65864459	1313343397	30321784529	799462887341
		23795492951147...			
78	397	2719	24509	280913	3965483
		67247771	1342401539	31023447269	818701472243
		24388288001989...			
80	409	2803	25423	292489	4142053
		70432519	1409422013	32644249103	863205467819
		25761357737977...			
81	419	2897	26371	304553	4326473
		73768631	1479780677	34349423377	910115902141
		27211243680073...			
82	421	2909	26489	305999	4348681
		74172503	1488302867	34556157661	915809403721
		27387388206553...			
84	433	3019	27689	321017	4578163
		78339559	1576442723	36697520357	974856473813
		29216297536511...			
85	439	3067	28109	326203	4658099
		79794157	1607252663	37447368857	995564440951
		29858589333061...			
86	443	3109	28573	332099	4748047
		81428323	1641908027	38291437141	1018893116299
		30582699050611...			
87	449	3169	29153	339601	4863959
		83543071	1686826109	39386748617	1049194449883
		31524064728311...			
88	457	3229	29803	347849	4989697
		85839547	1735649329	40578571003	1082201297941
		32550506359429...			
90	463	3299	30557	357473	5138719
		88565483	1793681753	41997140089	1121535591721
		33775078562347...			
91	467	3319	30781	360293	5182717
		89369047	1810798861	42415879469	1133155938589
		34137123380603...			
92	479	3407	31667	371981	5363167
		92678347	1881428537	44145738083	1181205761389
		35635464099689...			

Appendix 1

Matrix [$\overline{\mathbf{M}}$ $^{\mathbf{2}}$P]... Continuation 5.

93	487	3469	32341	380557	5496349
		95121911	1933651711	45426482839	1216826411041
		36747532444747...			
94	491	3517	32797	386401	5587537
		96797411	1969496239	46306458839	1241322670799
		37512927359291...			
95	499	3559	33203	391711	5670851
		98330021	2002298621	47112340151	1263771327193
		38214783465337...			
96	503	3593	33569	396269	5741453
		99630571	2030158657	47797243919	1282861540019
		38811965770483...			
98	521	3733	35023	415253	6037513
		105089261	2147305243	50681376121	1363360331743
		41333311232987...			
99	523	3761	35311	418961	6095731
		106166089	2170447637	51251887327	1379303865481
		41833278300773...			
100	541	3911	36887	439357	6415081
		112073683	2297602183	54391267121	1467155677657
		44591559921641...			
102	557	4027	38153	455849	6673993
		116881321	2401362767	56958606937	1539140110927
		46855727983837...			
104	569	4133	39239	470207	6898807
		121064467	2491797367	59200082443	1602086508713
		48838469899327...			
105	571	4153	39451	472837	6940103
		121834483	2508461203	59613478459	1613705610163
		49204743622123...			
106	577	4217	40151	481847	7081709
		124469621	2565499711	61029312569	1653521623993
		50460527025823...			
108	593	4339	41491	499403	7359427
		129647857	2677808011	63821022049	1732128413677
		52942646093899...			
110	601	4421	42293	510031	7528669
		132814411	2746597487	65533394977	1780407360517
		54468962620717...			
111	607	4463	42697	515401	7612799
		134389627	2780844971	66386576369	1804479121591
		55230488801623...			

Matrix [$\overline{\mathbf{M}}$ ^{2}**P**]... Continuation 6.

112	613	4517	43283	522829	7730539
		136593931	2828789699	67581794939	1838220650251
		56298481067219...			
114	619	4567	43889	530773	7856939...
115	631	4663	44879	543967	8066533...
116	641	4759	45971	558643	8300687...
117	643	4787	46279	562711	8365481...
118	647	4801	46451	565069	8402833...
119	653	4877	47297	576203	8580151...
120	659	4933	47857	583523	8696917...
121	661	4943	47963	584999	8720227...
122	673	5021	48821	596243	8900383...
123	677	5059	49207	601397	8982923...
124	683	5107	49739	608459	9096533...
125	691	5189	50591	619739	9276991...
126	701	5281	51599	633467	9498161...
127	709	5381	52711	648391	9737333...
128	719	5441	53353	657121	9878657...
129	727	5503	54013	665843	10020343...
130	733	5557	54601	673793	10147877...
132	743	5651	55681	688249	10382033...
133	751	5701	56197	695239	10493953...
134	757	5749	56701	702173	10606223...
135	761	5801	57193	708479	10707449...
136	769	5851	57751	715969	10829519...
138	787	6037	59723	742681	11261903...
140	809	6217	61819	771079	11723507...
141	811	6229	61979	773317	11760029...
142	821	6311	62921	786053	11967047...
143	823	6323	63059	788009	11999111...
144	827	6353	63391	792413	12071197...
145	829	6361	63467	793511	12089177...
146	839	6469	64679	809917	12356863...
147	853	6599	66089	828923	12667463...
148	857	6653	66749	838091	12816389...
150	863	6691	67157	843613	12907091...
152	881	6841	68821	866329	13280819...
153	883	6863	69109	870161	13343881...
154	887	6899	69491	875519	13431967...
155	907	7057	71287	900157	13836751...
.	.	.	.	.	.

References

[1] *L. Alexandrov,* "Multiple Eratosfhenes sieve and the prime number distribution on the plane", Sofia, 1964 (unpublished) .

[2] *Lubomir Alexandrov,* "On the nonasymptotic prime number distribution", e-print: math.NT/9811096, Nov., 1998 .

[3] *N.J.A Sloane and S. Plouffe,* "The Encyclopedia of Integer Sequences", Academic Press, San Diego, 1995 .

[4] *N.J.A Sloane,* "The On–Line Encyclopedia of Integer Sequences", http://www.research.att.com/~njas/sequences .

[5] *Jean-Pierre Chandeux and Alain Connes,* "Conversation of Mind, Matter, and Mathematics", Princeton University Press, 2000 .

[6] *T. Forbs,* "Prime Clusters and Cunningham Chains", Math. Comput. **68**, 1739–1749, 1999 .

[7] *F. Göbel,* "On 1–1–Correspondence between Rooted Trees and Natural Numbers", J. of Combinatorial Theory, series B **29**, 141–143, 1980 .

[8] *A. Odlysko, M. Rubinstein and M. Wolf,* "Jamping Champions", Experimental Math.,v. 8, No. 2, 107–118, 1999 .

[9] *Stein M.L., Ulam S. M. and Wells H. B.,* "A Visual Display of Some Properties of the Distribution of Primes", Amer. Math. Monthly **71**, 516–520, 1964 .

[10] *Adolf Hildebrand and Helmut Maier,* "Irregularities in the distribution of primes in short intervals", J. reine angew. Math. **397**, 162–193, 1989 .

[11] *L. Alexandrov, D. Karadjov,* "Method for the Approximate Solution of Eigenvalue Problems for Linear Differential Equations of a High Order", J. Comput. Math. and Math. Phys., 20, 4, 923–938, (1980, Russian).

[12] *Ronald L. Graham, Donald E. Knuth, Oren Patashnik,* "Concrete Mathematics", Addison–Wesley, Menlo Park, Ca, 1994 .

[13] *A. R. Conn, N. J. H. Gould and P. L. Toint,* "Trust-Region Methods", SIAM, MPS, Philadelphia, 2000 .